Geochemistry Geophysics Geosystems G3

Article
Volume 12, Number 5
7 May 2011
Q05002, doi:10.1029/2010GC003372
ISSN: 1525-2027

Published by AGU and the Geochemical Society

Nonhomogeneous seawater Sr isotopic composition in the coastal oceans: A novel tool for tracing water masses and submarine groundwater discharge

Kuo-Fang Huang
Earth Dynamic System Research Center, National Cheng Kung University, Tainan 701, Taiwan

Also at Department of Earth Sciences, National Cheng Kung University, Tainan 701, Taiwan

Now at Department of Geology and Geophysics, Woods Hole Oceanographic Institution, Woods Hole, Massachusetts 02543, USA (kfhuang05@gmail.com)

Chen-Feng You and Chuan-Hsiung Chung
Earth Dynamic System Research Center, National Cheng Kung University, Tainan 701, Taiwan

Also at Department of Earth Sciences, National Cheng Kung University, Tainan 701, Taiwan

In-Tian Lin
Department of Geosciences, National Taiwan University, Taipei 106, Taiwan

[1] Here we present high-precision (2σ = ±3 ppm) $^{87}Sr/^{86}Sr$ measurements in coastal waters, together with salinity, to evaluate water mass mixing and the influence of submarine groundwater discharge (SGD) in coastal waters and marginal seas. Nonhomogeneous Sr isotopic variations in water columns were documented in the Southern Okinawa Trough (SOT), South China Sea, and Kao-ping Canyon (KPC), where seawater $^{87}Sr/^{86}Sr$ varied up to 70 ppm. Seawater Sr isotopic composition changes only slightly in the upper 200 m of the SOT but was detectable and highly correlated with salinity, indicating a mixing between radiogenic North Pacific Tropical Water (high $^{87}Sr/^{86}Sr$ and high salinity) at 100–150 m and a less radiogenic component with low $^{87}Sr/^{86}Sr$ and low salinity at ~200 m. Vertical profiles of seawater $^{87}Sr/^{86}Sr$ along the KPC show significant variations, suggesting dynamic mixing affected by continental inputs (i.e., river runoff and SGD) in this region. These results highlight the potential use of seawater Sr isotopes as a powerful tracer for determining mixing ratios and the dynamic mixing of oceanic water masses, especially in coastal and marginal seas.

Components: 7700 words, 5 figures, 3 tables.

Keywords: seawater Sr isotope; water mass mixing; submarine groundwater discharge.

Index Terms: 1040 Geochemistry: Radiogenic isotope geochemistry; 1050 Geochemistry: Marine geochemistry (4835, 4845, 4850).

Received 22 September 2010; **Revised** 7 March 2011; **Accepted** 16 March 2011; **Published** 7 May 2011.

Huang, K.-F., C.-F. You, C.-H. Chung, and I.-T. Lin (2011), Nonhomogeneous seawater Sr isotopic composition in the coastal oceans: A novel tool for tracing water masses and submarine groundwater discharge, *Geochem. Geophys. Geosyst.*, *12*, Q05002, doi:10.1029/2010GC003372.

1. Introduction

[2] The Sr isotopic composition (Sr IC) of marine precipitates, such as biogenic and authigenic carbonates, has been widely used in global climate change studies and serves as a crucial tool for stratigraphic correlation and dating carbonate sequences [e.g., *Burke et al.*, 1982; *Dia et al.*, 1992; *Henderson et al.*, 1994]. These applications assume that Sr behaves uniformly both in chemical and isotopic distribution because of its much longer residence time (2–2.5 Myr) relative to the ocean mixing time scale (~10^3 yr) [*Basu et al.*, 2001]. The homogeneity of seawater Sr IC was also examined by $^{87}Sr/^{86}Sr$ in the Hudson Bay (S = 21.9), Pacific Ocean, Atlantic Ocean and Arctic Ocean [*Capo and DePaolo*, 1992; *Winter et al.*, 1997], as well as in marine carbonates [e.g., *Burke et al.*, 1982]. These published data suggest that open ocean Sr IC is spatially homogeneous, with no measurable variation at the analytical precision of 20–30 ppm (2σ) [*Henderson et al.*, 1994].

[3] Recent studies, however, have documented small but considerable regional differences in both Sr flux and Sr IC on time scales much shorter than the Sr residence time in the ocean [*Stoll and Schrag*, 1998; *de Villiers*, 1999], especially in the estuarine mixing zone and coastal ocean [*Andersson et al.*, 1994; *Xu and Marcantonio*, 2004; *Huang and You*, 2007]. These findings reflect recent advances in analytical precision over traditional Sr isotope techniques, and also highlight the need for a more detailed understanding of Sr geochemical cycling in the coastal oceans, and hence the oceanic Sr budget. Several potential mechanisms for causing the nonconservative behavior of Sr and Sr IC in the estuarine and coastal environments have been proposed in earlier works: (1) Sr scavenging by Fe-Mn oxyhydroxides [*Andersson et al.*, 1994], (2) intense water-sediment interaction [*Huang and You*, 2007], and (3) environmental disturbances causing compositional changes in the suspended and dissolved phases [*Xu and Marcantonio*, 2004]. These studies have highlighted that the $^{87}Sr/^{86}Sr$ isotopic ratio in coastal waters might deviate from that of contemporaneous seawater, and may influence the application of seawater Sr IC for stratigraphic dating purposes. On the other hand, these observations highlight the potential use of seawater Sr IC as a powerful tracer for identifying processes occurring between seawater and continental freshwater in the coastal oceans [*Huang and You*, 2007] because oceanic waters ($^{87}Sr/^{86}Sr$ = 0.709176) and continental freshwaters (e.g., $^{87}Sr/^{86}Sr$ = 0.741 in the Ganges catchment [*Bickle et al.*, 2003]) differ significantly in their Sr ICs.

[4] Detailed studies of Sr nonconservative behavior in the coastal oceans are scarce. In our earlier publication, small but distinguishable Sr isotopic variations (up to 50 ppm) were detected in coastal and estuarine environments after a typhoon event [*Huang and You*, 2007; *Lin et al.*, 2010]. The present study aims at exploring the use of seawater $^{87}Sr/^{86}Sr$ for tracing potential mixing processes among distinct water masses in marginal seas (i.e., Southern Okinawa Trough and South China Sea) and coastal regions (Kao-ping Canyon, Southwestern Taiwan). Toward this end, we present seawater Sr IC measurements of superior precision (±3 ppm, 2σ) coupled with conventional salinity measurements for a suite of depth profiles in the central and western Pacific. The potential use of seawater Sr IC for tracing continental inputs from closely situated rivers and water mass mixing offshore is systematically evaluated, in particular for regions where salinity variations among water masses are indistinguishable.

2. Methods

2.1. Sample Collection

[5] Seawater from three vertical profiles in the Southern Okinawa Trough (SOT) were sampled during the R/V *Ocean Researcher* I-679 expedition in April 2003 (Figure 1b), and used for studying water mass mixing of the Kuroshio Current near Taiwan. Four depth profiles along the Kao-ping Canyon (KPC) were collected during the R/V *Ocean Researcher* III-720 expedition in August 2001, approximately 1 week after Typhoon Toraji, to investigate the influence of continental inputs, such as river runoff and SGD. Three reference sites, ST-1 (10°N, 140°W) and SB-09 (34.13°N, 120.02°W) located at the North Equatorial Current (NEC) and California Borderland, respectively, as well as SCS-C (15°N, 115°30′E) in the central South China Sea (SCS), were analyzed for comparison (Figure 1a).

[6] Immediately after sampling through Niskin bottles (X type) deployed on a Rosette assembly, the sample was filtered through a 0.45 μm membrane, transferred to trace metal clean HDPE containers and prevented from freezing during transit and storage. Water samples for seawater Sr IC, dissolved Ba and Mn determinations were acidified to pH~1.5 using subboiled quartz distilled HNO_3 on board.

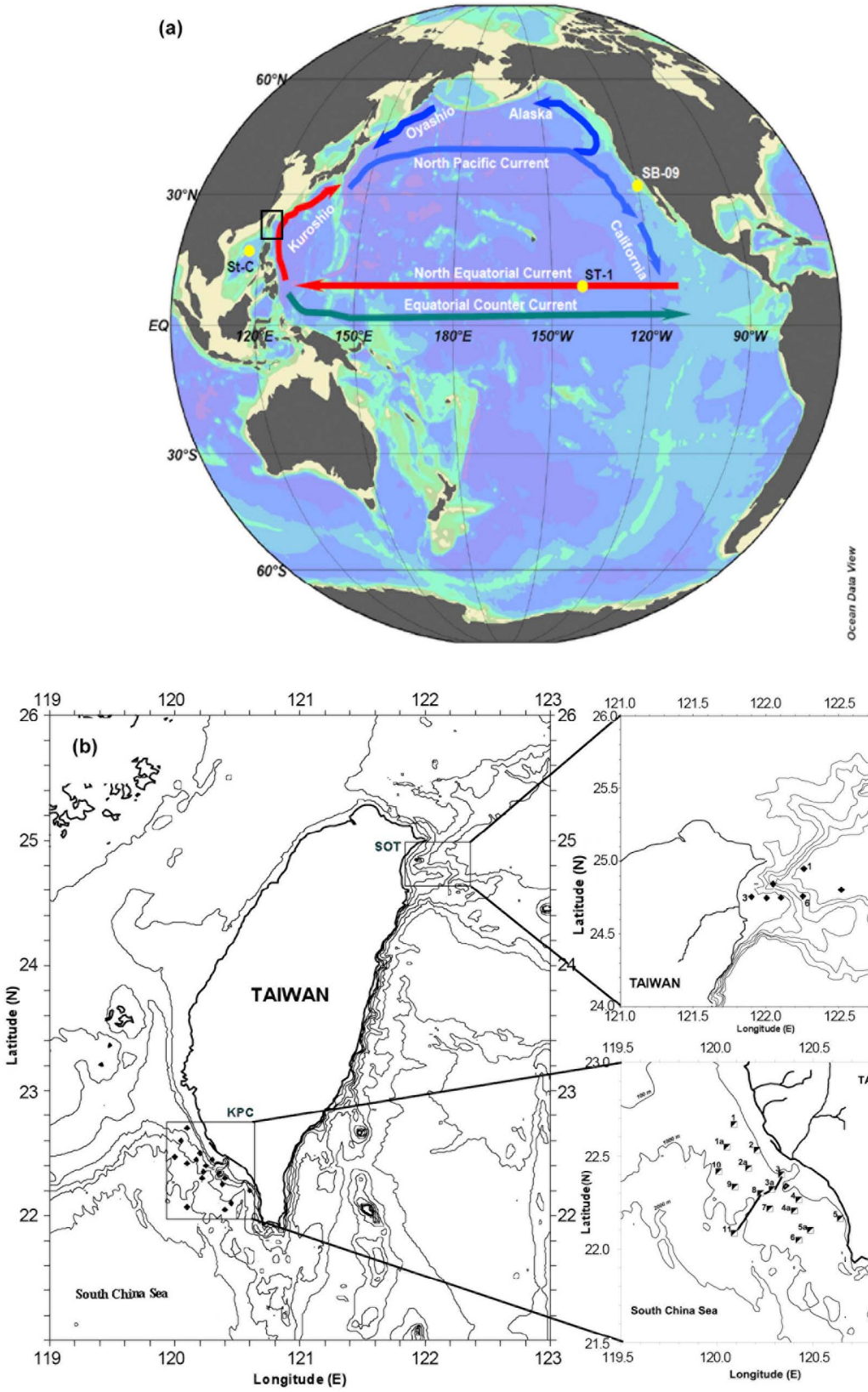

Figure 1. Locations of seawater sampling stations in the (a) North Pacific and the (b) SOT and KPC transects around Taiwan.

Temperature and salinity were measured using a Sea-Bird Electronics SBE 9/11 plus CTD Conductivity, and the uncertainty for salinity is within ±0.01.

2.2. Analytical Method

[7] The Sr separation procedures used in this study were modified from *Deniel and Pin* [2001]. In the laboratory, Sr was purified under a class 10 flow bench. For Sr IC analyses, 0.1 mL of seawater containing 700–800 ng Sr was passed through Sr^{SPEC} resin (Eichrom™, 1 mL) and the elutant (in 0.05N HNO_3) was evaporated to dryness and redissolved in 0.1N HCl. Total procedure blanks of Sr were 10–20 pg and are negligible compared with the loading size. The purified Sr was then loaded onto double Ta/Re filaments, and Sr isotope ratios were measured using a static mode Thermal Ionization Mass Spectrometer (Thermo-Fisher Scientific Triton TI) installed at EDSRC, NCKU. The ^{88}Sr beam was held at 200 pA for 1 h and 135 ratios with 15 blocks were collected. Mass fractionation and Rb contribution were corrected by $^{86}Sr/^{88}Sr$ normalization to 0.1194 applying an exponential law and the natural $^{85}Rb/^{87}Rb$ abundance, respectively. Replicate analyses of NBS 987, $^{87}Sr/^{86}Sr$ = 0.710270 ± 03 (2σ, n = 25) show an excellent long-term reproducibility of better than 3 ppm. However, standard reproducibility does not account for variability in natural samples due to matrix effects or interferences. Therefore, six seawater duplicates from the North Pacific were also carried out and further confirmed that analytical reproducibility for the natural seawater is similar to the long-term precision and within-run precision (<3 ppm). This technique thus enables us to examine small natural variability in coastal waters [*Huang and You*, 2007]. In the following discussion, the seawater Sr IC is expressed as the ppm deviation from that of deep North Pacific seawater.

$$\Delta^{87}Sr = \left(\frac{\left(\frac{^{87}Sr}{^{86}Sr}\right)_{sample}}{\left(\frac{^{87}Sr}{^{86}Sr}\right)_{STD}} - 1 \right) \times 10^6 (ppm)$$

where STD represents the present-day seawater in the deep North Pacific Ocean, $^{87}Sr/^{86}Sr$ = 0.709176 ± 03, which is identical within error to the deep water of the SCS (0.709180 ± 03).

[8] Dissolved Ba and Mn of the estuarine waters were directly determined using 200-fold dilution samples by high-resolution inductively coupled plasma mass spectrometry (HR-ICP-MS, Thermo-Fisher Scientific Element 2) at EDSRC, NCKU. A series of matrix-matched standards prepared from certified seawater reference materials, NASS-5 (National Research Council Canada, salinity = 30.4) and CASS-4 (National Research Council Canada, salinity = 30.7), were used to correct for potential matrix-induced mass discrimination. Estimates of analytical precision and accuracy for dissolved Ba and Mn based upon analyses of the standards are on the order of 5%. Detection limit is 5 ppt and 10 ppt for dissolved Ba and Mn, respectively.

3. Hydrography and Water Mass

3.1. North Pacific

[9] The major features of the surface circulation in north Pacific are (1) large anticyclonic gyres with axes along 20°N and (2) the equatorial current system [*Reid*, 1997]. The North Equatorial Current (NEC) is the parental water mass of the North Pacific Tropical Water (NPTW) and Kuroshio Current (KC). The NEC flows westward between 12 and 13°N, and breaks into two branches, the northward KC and southern Mindanao Current, near the Luzon Island. Although the KC originates from the NEC, the chemical composition between the KC and NEC may be significantly altered due to exchange with volcanic materials in the Luzon Arc [*Tomczak and Godfrey*, 1994]. The KC flows northward and joins the North Pacific Current, which is the upper stream of the California Current (Figure 1a).

[10] The water masses of the intermediate and deep North Pacific Ocean were described by *Tomczak and Godfrey* [1994] as Subarctic Intermediate Water or North Pacific Intermediate Water (NPIW) and Pacific Deep Water (PDW). The salinity minimum near 800–1000 m depth indicates the present of this intermediate water. NPIW originates from the Polar Front, where it is formed by mixing of surface and deeper waters and subducted into the subtropical gyre. The constituents of PDW are North Atlantic Deep Water, Antarctic Bottom Water and Antarctic Intermediate Water.

3.2. South Okinawa Trough

[11] The Kuroshio Current, a major western boundary current in the Pacific, consists of the following well-defined components at depths shallower than 1500 m [*Chen et al.*, 1995]. In the SOT region, the major water masses and their hydrological properties are: Kuroshio Surface Water, with the highest temperature (>25°C) and pH, and depleted

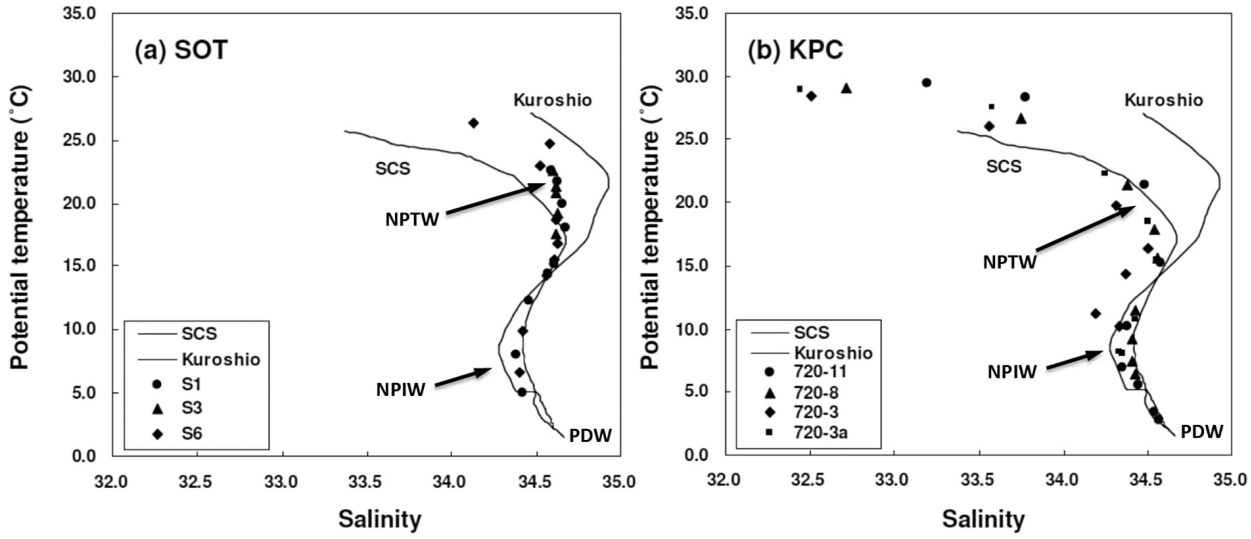

Figure 2. The θ-S diagram showing distributions of water samples in the (a) SOT and (b) KPC. The typical curves of the SCS and KC proper waters are also shown for comparison [*Lin et al.*, 2010].

in nutrients and alkalinity; NPTW, characterized by high nutrients and alkalinity, as well as a subsurface salinity maximum ~34.9 (σ_θ = 23) at 100 to 200 m (shallower in winter and deeper in summer), and originating from the northward branch of the NEC; NPIW occupies depths between 400 and 1500 m, marked by a salinity minimum (34.2, σ_θ = 26.7) at ~490 m [*Nitani*, 1972] and most likely forms by a shortcut of Okhotsk Sea source water into the western subtropical gyre [*You*, 2003]. The layer immediately beneath NPIW is occupied by the nutrient-depleted PDW. At depths greater than 2000 m, temperature and salinity are rather uniform (θ = 1.1–1.8°C and S = 34.6–34.7) [*Amakawa et al.*, 2004]. Figure 2a shows the potential temperature-salinity diagrams at three stations investigated in this study. The θ-S plot clearly defines the water masses in the SOT, such as the NPTW, NPIW and PDW.

3.3. South China Sea and Kao-ping Submarine Canyon

[12] The distributions of water masses at the KPC are rather complicated due to intense regional mixing of multiple source waters from on-land Taiwan. Several water masses were identified near the KPE and the SCS based on hydrographic measurements [*Nitani*, 1972]. The Kao-ping River Water carries a large amount of fresh runoff and precipitation with salinity values close to zero and occupies predominantly the surface layer during prevailing summer monsoon seasons. The South China Sea Surface Water transports waters from the SCS and could be strongly influenced by surface circulation due to annually reversing monsoon winds. Due to intensive upwelling and vertical mixing, the salinity extremes in this region are less pronounced than in the SOT, i.e., NPTW has a maximum salinity of 34.65 centered at ~150 m deep, and NPIW has a minimum salinity of 34.4 at around 500 m [*Chou et al.*, 2007]. In the deep SCS, the Luzon Strait (~2600 m) serves as the only gateway of deep water exchange between the SCS and deep Pacific water. All SCS waters below 1500 m display similar hydrographic properties (e.g., θ and S) as that of the Pacific at 2000 m, except at 1500 m where a slightly high T occurred [*Chen et al.*, 2006]. The θ-S plot clearly shows the water masses in the KPC and the SCS, including surface water, NPTW, NPIW and PDW (Figure 2b).

4. Results and Discussion

4.1. Vertical Distribution of Sr IC in the North Pacific

[13] The depth profile of seawater Δ^{87}Sr in the California Borderland, SB-09, shows <10 ppm variation within the upper 500 m; in contrast, the vertical Δ^{87}Sr profile in the open ocean station, ST-1, displays a nonhomogeneous pattern, ranging from 0 to +37 ppm (Figure 3a and Table 1). More radiogenic Δ^{87}Sr (~+20 ppm) at depths of 100–150 m (occupied by NPTW) and 400–600 m (dominated by NPIW) are detected, and can be used to represent the Sr isotopic signatures of the KC water masses. It is interesting to note that a similar

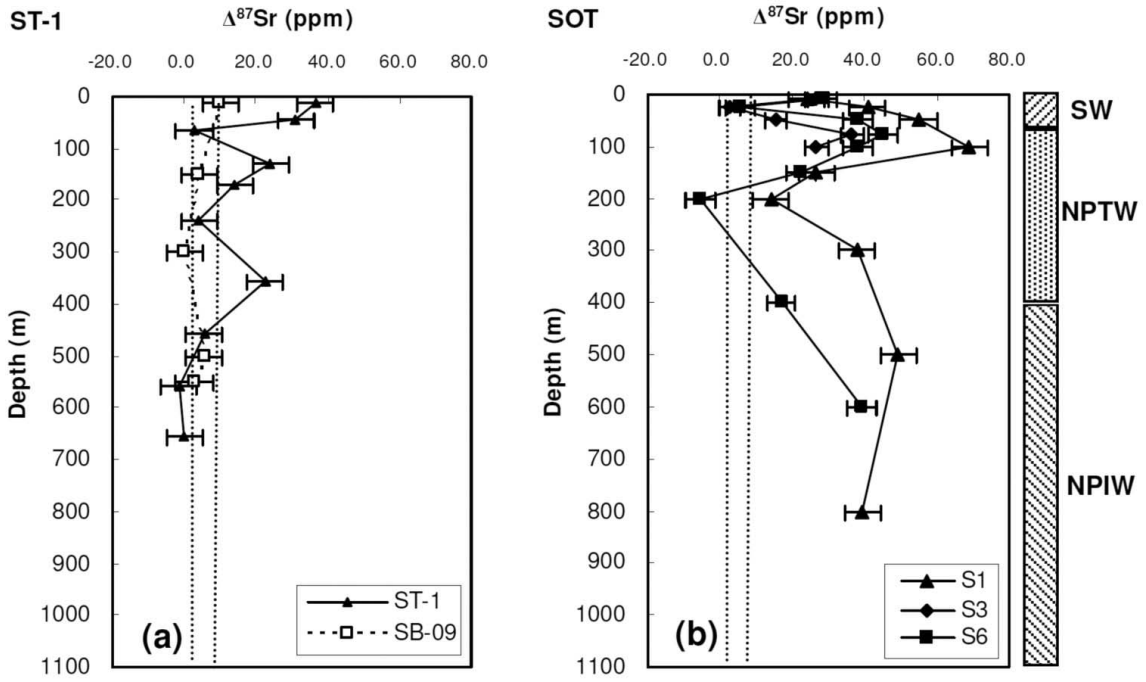

Figure 3. (a) Depth distributions of seawater Sr IC at the open ocean sites, ST-1 and SB-09, located in the North Pacific. (b) Depth profiles of seawater Sr IC in the SOT. Note that the dashed lines represent the range of Δ^{87}Sr in the deep Pacific water.

feature has also been observed in vertical profiles of seawater Nd isotopes (ε_{Nd}) in subtropical North Pacific stations [*Amakawa et al.*, 2004, 2009]. In these studies, the unradiogenic ε_{Nd} for NPTW had been attributed to the influence of a continental source from shelf sediments (with unradiogenic ε_{Nd} and radiogenic Δ^{87}Sr) of the East China Sea. This is clearly consistent with the more radiogenic Δ^{87}Sr characteristic of NPTW presented here. In addition, within the first 50 m Δ^{87}Sr is higher (ST-1: Δ^{87}Sr = +37 ppm at 11.6 m; SB-09: Δ^{87}Sr = +10 ppm at 11 m) than in the deeper waters. This can be attributed to input of windblown dust from eastern Asia, such as the Chinese Loess Plateau and Mongolian region. It has been suggested that dust-derived Sr could significantly modify seawater Sr and Δ^{87}Sr toward a higher and more radiogenic value via dissolution of long-range transport eolian calcite and silicate dust [*Jacobson*, 2004]. It could therefore be valuable to evaluate possible contributions of continental dust, which provides a quantitatively significant source of Sr to surface seawater.

[14] Recent estimates for the soluble calcite dust flux from eastern Asian to the North Pacific is ~5 × 10^{13} g/yr [*Jacobson*, 2004] (or 0.6 g/m^2/yr, assuming surface area of the North Pacific is 80 × 10^6 km^2, half of the Pacific). Consideration of only the carbonate fraction, with a presumed Sr content of ~1500 μg/g and ^{87}Sr/^{86}Sr = 0.711 [*Jacobson*, 2004], equates to a Sr dust flux of ~11 μmol/m^2/yr if complete dissolution of eolian calcite occurred. Assuming no other process adds or removes seawater Sr, a simple mass balance indicates that it would take ~70 years to produce a 0.75 μmol/kg change in Sr per meter depth in the upper ocean (corresponding to a ~+20 ppm change in Δ^{87}Sr), similar to a previous estimate for the contribution of Saharan dust to Atlantic Ocean [*de Villiers*, 1999]. *de Villiers* [1999] reported a rather small change (<0.1 μmol/kg) in the upper 90 m of North Pacific (45°N, 179°E), corresponding to a <0.001 μmol/kg decrease in Sr per meter depth. On the basis of this simple calculation, <0.1 year is needed to generate the observed variation, suggesting that dust inputs from eastern Asia can significantly influence ocean surface Sr and Sr IC in the North Pacific.

[15] At depth intervals of 120–150 m and 400–450 m, Δ^{87}Sr displays more radiogenic values of ~+25 ppm relative to the deep ocean. The isotopically heavy Sr IC, a unique feature of the region, could be related to the nature of two major water masses, NPTW and NPIW, in the study area. A previous study showed that seawater Sr has a semi-conservative nature in both the Pacific and Atlantic

Table 1. Sr Isotope and Hydrographic Data Measured in Seawaters in the North Pacific and SOT[a]

Station	Latitude	Latitude	Depth (m)	T	S	$^{87}Sr/^{86}Sr$	2 SE	$\Delta^{87}Sr$ (ppm)
ST-1	10°N	140°W	12	–	–	0.709202	3	36.7
			43	–	–	0.709198	3	31.0
			64	–	–	0.709178	2	2.8
			128	–	–	0.709193	2	24.0
			168	–	–	0.709186	3	14.1
			238	–	–	0.709179	2	4.2
			357	–	–	0.709192	2	22.6
			458	–	–	0.709180	3	5.6
			558	–	–	0.709175	3	−1.4
			657	–	–	0.709176	3	0.0
SB-09	34°N–13.43°N	120°W–01.91°W	11	–	–	0.709183	2	9.9
			150	–	–	0.709179	2	4.2
			300	–	–	0.709176	2	0.0
			500	–	–	0.709180	3	5.6
			550	–	–	0.709178	3	2.8
679-S1	24°N–56.91°N	122°E–15.62°E	10	22.62	34.58	0.709193	2	24.0
			10[b]	22.62	34.58	0.709195	2	26.8
			25	21.70	34.62	0.709205	1	40.9
			50	19.95	34.66	0.709215	2	55.0
			100	18.10	34.67	0.709225	2	69.1
			150	15.17	34.61	0.709195	3	26.8
			200	14.40	34.57	0.709186	4	14.1
			300	12.25	34.46	0.709203	2	38.1
			500	8.01	34.38	0.709211	2	49.4
			800	5.04	34.42	0.709204	1	39.5
679-S3	24°N–45.22°N	121°E–54.00°E	10	22.61	34.60	0.709195	2	26.8
			10[b]	22.61	34.60	0.709195	3	26.8
			25	21.38	34.61	0.709178	2	2.8
			50	20.76	34.62	0.709187	2	15.5
			75	19.21	34.63	0.709202	3	36.7
			100	17.61	34.61	0.709195	3	26.8
679-S6	24°N–45.45°N	122°E–15.28°E	25	24.75	34.58	0.709180	4	5.6
			50	22.95	34.52	0.709203	3	38.1
			75	18.66	34.61	0.709208	2	45.1
			100	16.76	34.63	0.709203	2	38.1
			150	15.54	34.61	0.709192	2	22.6
			200	14.26	34.56	0.709172	5	−5.6
			200[b]	14.26	34.56	0.709174	3	−2.8
			200[b]	14.26	34.56	0.709175	3	−1.4
			400	9.90	34.42	0.709188	3	16.9
			600	6.60	34.40	0.709204	2	39.5
			600[b]	6.60	34.40	0.709202	3	36.7

[a]Uncertainties for $^{87}Sr/^{86}Sr$ measurements are shown as 2 SE (n = 135), and long-term reproducibility for NBS 987 is 3 ppm. $\Delta^{87}Sr$ are calculated using a seawater value of 0.709176 in the deep North Pacific.
[b]Duplicated seawater samples.

Oceans [*de Villiers*, 1999]. They highlighted that potential mechanisms for the pronounced upper ocean dissolved Sr gradient were related to remineralization (e.g., celestite produced by surface-dwelling acantharia) associated with biogenic fluxes in the upper ocean [*Brass and Turekian*, 1974] and dissolution of celestites or biogenic calcium carbonates in the surface ocean [*Bernstein et al.*, 1987, 1992].

[16] In general, heavy isotopes tend to be enriched in phases where the element forms the strongest bonds [*Schauble*, 2004], implying that the observed Sr isotopic variations in the seawaters could perhaps be due to such biomineralization/dissolution processes in the water column. However, this interpretation needs to be further verified with independent evidence to gain a better constraint on the variability in seawater Sr IC through the above processes. For example, a sediment trap study might be helpful for understanding the spatial and temporal variability in acantharia fluxes, and would aid in further quantitative estimation of Sr isotope fractionation in the ocean.

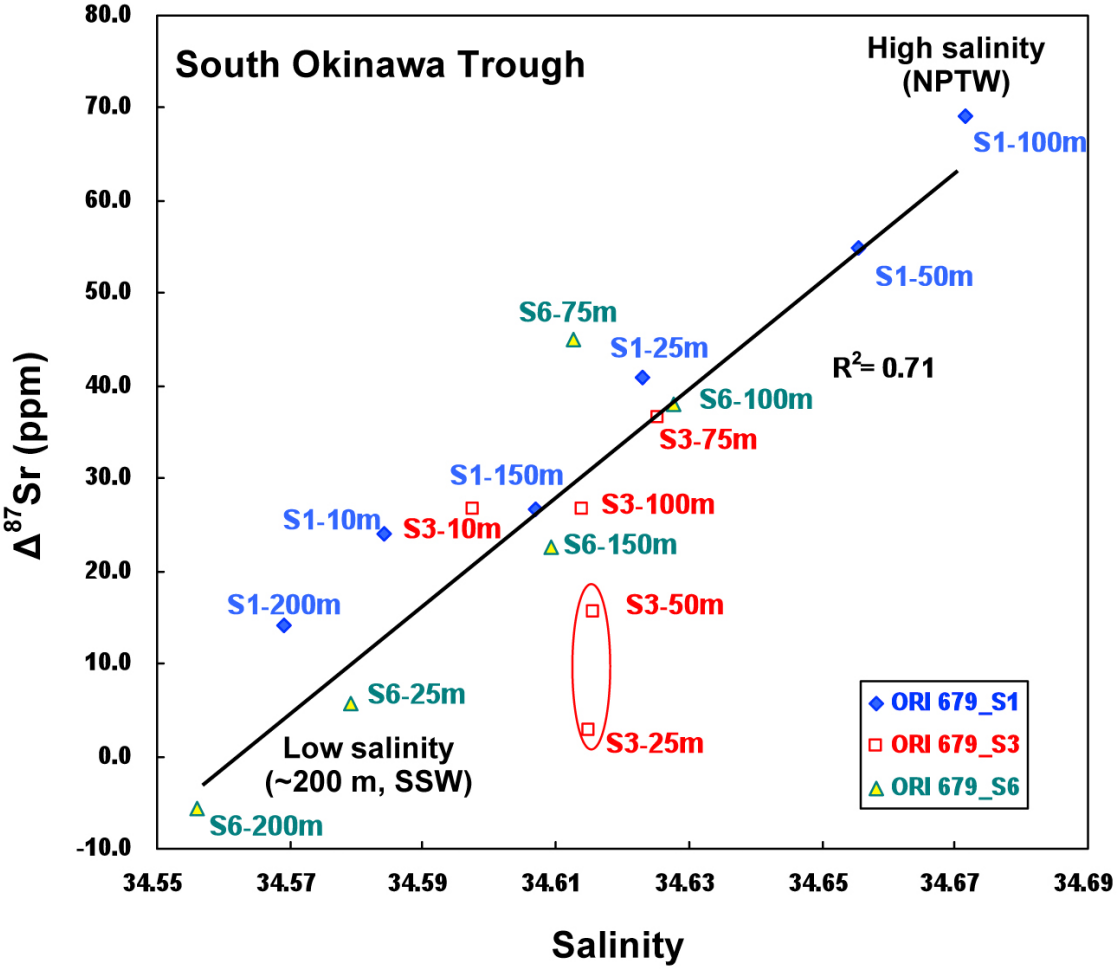

Figure 4. Seawater $\Delta^{87}Sr$ versus salinity plot illustrating the potential two end-member (i.e., high-salinity NPTW and low-salinity SSW) mixing regime between the more radiogenic and less radiogenic source waters in the SOT.

4.2. Vertical Distribution of Sr IC in the SOT

[17] Radiogenic $\Delta^{87}Sr$ values of 24–28 ppm are observed in the surface waters of the SOT (Figure 3b), demonstrating the significant influence of eolian dust from eastern Asia. Since the KC is the main water mass in this area, the vertical structure of Sr IC should be analogous to the reference site, ST-1, located at the formation region of the KC (i.e., the NEC). In Figure 3b, depth profiles of seawater Sr IC in the SOT show a rather similar distribution pattern, characterized by more radiogenic $\Delta^{87}Sr$ at the surface layer and at depths 100–150 m and 400–600 m, clearly depicting the characteristics of the KC water masses in the SOT region. In comparison with the KC water masses at ST-1 (see Figure 1a), potential sources of more radiogenic Sr IC at depths 100–150 m and 400–600 m are still poorly constrained in this study. However, additional input of SCS subsurface water outflow could modify the chemistry of KC water off southeastern Taiwan [*Chou et al.*, 2007], thus adding extra complication to the vertical structure of Sr IC in the SOT.

[18] In spite of the potential complexity in chemical properties of seawaters around Taiwan, distributions of seawater Sr IC clearly display a systematic pattern in the upper 200 m of the SOT. In Figure 4, a two end-member mixing trend ($r^2 = 0.96$, excluding the nearshore station ORI-679_S3) with characteristic $^{87}Sr/^{86}Sr$ derived from two sources can be observed on the $\Delta^{87}Sr$ and salinity plot. Sr isotope ratios and relevant hydrographic features of the two source components are (1) more radiogenic $^{87}Sr/^{86}Sr$ with relatively high salinity at depth ~100 m, which is related to the NPTW and (2) less radiogenic $^{87}Sr/^{86}Sr$ with a slightly lower salinity at depth ~200 m. It is worth noting that the salinity change in this region is less than 0.12; however, the variation

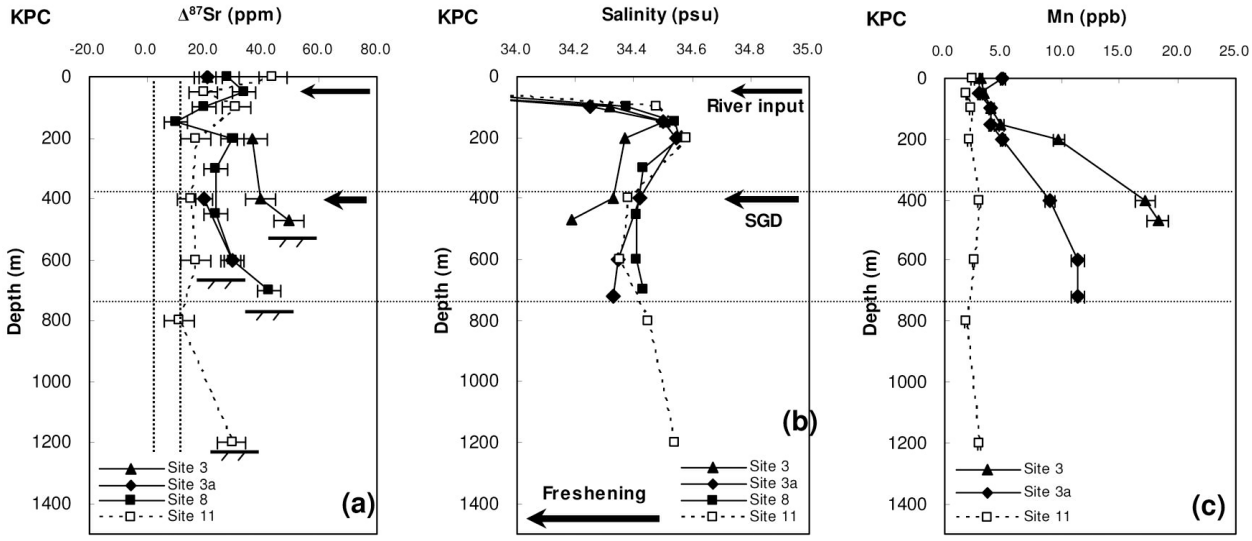

Figure 5. Depth profiles of (a) seawater Sr IC (adapted from *Lin et al.* [2010], copyright 2010, with permission from Elsevier), (b) salinity along the KPC transect, and (c) Mn in the coastal waters along the KPC transect in summer 2001, 1 week after the typhoon event. The vertical dashed lines show the range of the Δ^{87}Sr in the deep SCS water, and the bottom depths of the sampling sites are also marked. The horizontal dashed lines represent the depth range of the potential influence of the SGD (~400–700 m).

in seawater Sr IC can be >70 ppm, compared with 3 ppm (2σ) analytical error, suggesting that seawater Sr IC is much more sensitive than traditional tracers, such as salinity. This observation also demonstrates that Sr behaves conservatively in the coastal ocean. Thus, the simplified two end-member mixing model documented for the SOT strongly supports the application of Sr isotopes for tracing water masses and estimation of mixing ratios in the coastal region. Two Δ^{87}Sr data points from station ORI-679_S3 near the river mouth deviate slightly from the simple mixing trend, which could be explained by potential complications associated with the estuarine environment, such as precipitation of Fe-Mn oxide coating and/or sediment-water interaction [*Huang and You*, 2007].

4.3. Vertical Distribution of Sr IC in the SCS and KPC

[19] The Sr IC in the central SCS and the KPC are not distributed homogeneously (Figure 5 and Table 2). Vertical transects along the KPC, stations 3, 3a, 8 and 11, clearly depict unique characteristics of different water masses in KPE after a typhoon event. For the uppermost 100 m, Sr IC shows a more radiogenic (>20 ppm) signal than the deep SCS. This phenomenon is attributed to the addition of heavy Δ^{87}Sr related to continental input [*Huang and You*, 2007]. At 100–150 m, Sr IC displays large differences in station 8 and SCS-C, possibly caused by the KC intrusion [*Qu et al.*, 2000] and further mixing with SCS subsurface waters. The unique Sr IC distributions make it a novel tracer for monitoring freshwater migration in the coastal zone.

[20] At 400–700 m, a strong correlation exists between seawater Sr IC and relative distance from the river mouth, with ^{87}Sr/^{86}Sr becoming less radiogenic away from the estuary. At station 11, Δ^{87}Sr values are identical to deep water in the central SCS, suggesting negligible continental inputs. At depths greater than 800 m, Sr IC should be close to the deep SCS or NPIW. The Δ^{87}Sr at 1200 m is, however, ~20 ppm higher than the deep waters (see *Lin et al.* [2010] for detailed description). Contribution via SGD (e.g., recycled seawater) at depths >1000 m (e.g., offshore New Jersey [*Robb*, 1984]) is likely to have occurred. Alternatively, more intense water-sediment interaction associated with bottom resuspension may cause slightly heavy Sr ICs.

[21] There are two Δ^{87}Sr-enriched layers along the KPC at intervals 400–700 m and 1200 m (Figure 5a). In particular, Δ^{87}Sr at 400–700 m shows the largest enrichment (~+50 ppm) at station 3. At other stations (i.e., 3a and 8), the Sr IC is at least 20 ppm higher than at station 11. This scenario is consistent with an addition of greater continental freshwater to the nearby estuary stations, indicating that the flood event associated with the typhoon might affect SGD activity at least 25 km offshore. This agrees well with results from *Lin et al.* [2010],

Table 2. Sr Isotope and Dissolved Mn, as Well as Hydrographic Data Measured in Seawaters in the SCS and KPC[a]

Station	Latitude	Latitude	Depth (m)	T	S	$\delta^{18}O$	$^{87}Sr/^{86}Sr$	2 SE	$\Delta^{87}Sr$ (ppm)	Mn (ppb)
SCS-C	18°N	115°E–30.0°E	0	–	–	–	0.709204	3	39.5	–
			5	–	–	–	0.709202	3	36.7	–
			50	–	–	–	0.709188	3	16.9	–
			100	–	–	–	0.709209	2	46.5	–
			200	–	–	–	0.709184	1	11.3	–
			400	–	–	–	0.709183	3	9.9	–
			700	–	–	–	0.709180	3	5.6	–
			1000	–	–	–	0.709180	3	5.6	–
			1400	–	–	–	0.709180	2	5.6	–
720-3	22°N–23.84°N	120°E–20.05°E	0	28.50	32.5	−0.29	0.709191	1	21.2	3.10
			50	26.02	33.6	−0.04	–		–	3.37
			100	19.80	34.3	0.13	–		–	3.99
			150	16.32	34.5	0.14	–		–	4.86
			200	14.33	34.4	0.14	0.709202	3	36.7	9.76
			400	10.17	34.3	0.16	0.709204	2	39.5	17.2
			470	11.19	34.2	−0.07	0.709211	2	49.4	18.3
720-3a	22°N–19.16°N	120°E–17.12°E	0	28.90	32.4	−0.48	0.709191	2	21.2	5.00
			0[b]	28.90	32.4	−0.48	0.709192	2	22.6	5.00
			50	27.56	33.6	0.13	–		–	3.10
			100	22.25	34.3	0.17	–		–	4.10
			150	18.50	34.5	0.27	–		–	4.21
			200	15.52	34.5	0.29	–		–	5.00
			400	10.72	34.4	0.09	0.709190	3	19.7	9.00
			600	8.10	34.3	−0.02	0.709197	2	29.6	11.4
720-8	22°N–17.91°N	120°E–13.54°E	0	29.05	32.7	−0.37	0.709196	3	28.2	–
			50	26.71	33.7	0.00	0.709200	2	33.8	–
			100	21.45	34.4	−0.11	0.709190	3	19.7	–
			150	17.93	34.5	0.23	0.709183	3	9.9	–
			200	15.58	34.6	0.19	0.709197	3	29.6	–
			300	11.51	34.4	0.11	0.709193	2	24.0	–
			450	9.21	34.4	−0.02	0.709193	3	24.0	–
			600	7.37	34.4	−0.08	0.709197	3	29.6	–
			700	6.39	34.4	0.01	0.709206	4	42.3	–
720-11	22°N–05.04°N	120°E–05.34°E	0	29.49	33.2	−0.12	0.709207	2	43.7	2.44
			50	28.31	33.8	−0.12	0.709190	2	19.7	1.89
			100	21.34	34.5	0.19	0.709198	1	31.0	2.26
			200	15.29	34.6	0.23	0.709188	3	16.9	2.15
			400	10.21	34.4	−0.02	0.709187	3	15.5	2.95
			600	6.96	34.4	−0.04	0.709188	2	16.9	2.48
			800	5.54	34.4	−0.11	0.709184	3	11.3	1.86
			1200	3.35	34.5	−0.18	0.709197	3	29.6	2.99
			1600	2.81	34.6	−0.08	–		–	3.38

[a]Oxygen isotopes were obtained from *Lin et al.* [2010]. Uncertainty for $^{87}Sr/^{86}Sr$ measurements are shown as 2 SE (n = 135), and long-term reproducibility for NBS 987 is 3 ppm. $\Delta^{87}Sr$ are calculated using a seawater value of 0.709176 in the deep North Pacific Ocean.
[b]Duplicated seawater samples.

who found characteristically light $\delta^{18}O$ and rather low salinity (~0.2 lower than station 11, see Figure 5b) at the same layers. Moreover, dissolved Ba (shown by *Lin et al.* [2010]) and Mn in the nearshore stations (i.e., stations 3 and 3a) also display large enrichments at ~400–700 m depth relative to station 11 (Figure 5c), further supporting the argument of freshwater influence from the continent [*Moore*, 1997; *Huang and You*, 2007]. The combined results of Sr IC, salinity, and dissolved Ba and Mn suggest strong SGD from deep aquifers in Pingtung Plain, which serve as a freshwater source at depth near the KPC. This study demonstrates that SGD may discharge freshwater directly into the coastal zone apart from recycled brackish water [*Moore*, 1996]. On the other hand, NPIW at 400–1500 m in the northern SCS (i.e., SCS-C) may have modified Sr ICs in the deeper KPC. The $\Delta^{87}Sr$ along the KPC, however, displays a large difference at depth 400–700 m between the KPC and deep SCS (Figure 5), indicating that more radiogenic $\Delta^{87}Sr$ waters at 400–700 m cannot be attributed to NPIW. Also, the radiogenic seawater Sr IC observed at 400–700 m in the KPC is not consistent with the

Table 3. Mixing Ratios of the Upper 200 m of the SOT Based on Salinity and Seawater Sr IC Using the Simplified Mass Balance Calculation

Station	Latitude	Latitude	Depth (m)	S	Δ^{87}Sr (ppm)	Salinity-Based R_{mix}[a] (NPTW Fraction)	Sr IC-Based R_{mix}[b] (NPTW Fraction)
679-S1	24°N–56.91°N	122°E–15.62°E	10	34.60	24.0	0.36	0.39
			25	34.62	40.9	0.57	0.62
			50	34.66	55.0	0.87	0.81
			100	34.67	69.1	1.02	1.00
			150	34.61	26.8	0.45	0.43
			200	34.58	14.1	0.19	0.26
679-S3	24°N–45.22°N	121°E–54.00°E	10	34.60	26.8	0.34	0.43
			25	34.61	2.8	0.50	0.11
			50	34.62	15.5	0.51	0.28
			75	34.63	36.7	0.59	0.56
			100	34.61	26.8	0.49	0.43
679-S6	24°N–45.45°N	122°E–15.28°E	25	34.58	5.6	0.17	0.14
			75	34.62	45.1	0.58	0.68
			100	34.63	38.1	0.62	0.58
			150	34.61	22.6	0.45	0.37
			200	34.56	−5.6	0.00	0.00

[a]The uncertainty for salinity-based R_{mix} is estimated to be ±0.09.
[b]The uncertainty for Sr IC-based R_{mix} is estimated to be ±0.04.

expected unradiogenic Δ^{87}Sr for NPIW in the North Pacific due to the influence of the Oyashio Current (characterized by radiogenic Nd and unradiogenic Sr) [*Amakawa et al.*, 2004, 2009].

4.4. Mixing of Coastal Waters in the Southern Okinawa Trough Based on Salinity–Sr Isotope Mass Balance

[22] To validate the use of seawater Sr IC as a tracer, salinity and seawater Sr isotope measurements were combined to calculate the composition of the samples collected from the upper 200 m of the SOT in April 2003. As described in section 4.2, the upper SOT coastal waters can be assumed to contain a mixture of two end-members: saline NPTW (at water depth 100 m, S = 34.67 and Δ^{87}Sr = +69 ppm) and low salinity subsurface seawater (SSW, at 200 m, S = 34.56 and Δ^{87}Sr = −5 ppm). The salinity and Δ^{87}Sr values for the two saline end-members can be used to recalculate R_{mix}, a mixing ratio of NPTW to SSW, based on a simplified mass balance constraint listed in equations (1) and (2):

$$S_S = S_{NPTW} * R_{mix} + S_{SSW} * (1 - R_{mix}) \quad (1)$$

$$\Delta^{87}Sr_S = \Delta^{87}Sr_{NPTW} * R_{mix} + \Delta^{87}Sr_{SSW} * (1 - R_{mix}) \quad (2)$$

The calculated mixing ratios based on salinity and seawater Sr IC for each station are listed in Table 3, showing that the mixing proportions estimated from the two independent conservative tracers are in agreement with each other, except for the data from station 679_S3, which is near the river mouth. For example, on the basis of equation (1), the R_{mix} (NPTW fraction) of subsurface water sample, 679_S1–150 m (S = 34.61), is estimated to be 0.45, 45% NPTW and 55% SSW based on salinity. Using the estimated R_{mix} and equation (2), the calculated $\Delta^{87}Sr_S$ is +28 ppm, which is remarkably consistent with the measured Δ^{87}Sr value (+27 ppm). This simple evaluation further corroborates the validity of our modeled calculation using seawater Sr IC for tracing water mass mixing around the coastal ocean. This novel water mass tracer, however, would be restricted if water masses have very similar $^{87}Sr/^{86}Sr$ values (i.e., the variation is less than analytical precision of ±0.000003) in the study area.

4.5. Determination of the Contributions of the Submarine Groundwater Discharge Along the Kao-ping Canyon Based on Salinity and Sr IC Measurements

[23] After an episodic flood event, the dominant water mass at the surface KPC is Kao-ping River Water (KPRW). The KPRW carries a large amount of continental runoff with Δ^{87}Sr = 5347 ppm ($^{87}Sr/^{86}Sr$ = 0.712968) and salinity close to zero, occupying predominantly the surface layer and further mixed with coastal seawaters around the KPE [*Huang and You*, 2007]. At greater depth (as shown in Figure 5), the fresh SGD can be an important source of dissolved materials, such as trace elements (e.g., Mn and Ba) and nutrients, to the coastal ocean [*Moore*, 1997]. This is supported by the observed changes in salinity at the KPC

(Figure 5b) and is in agreement with recent numerical modeling and hydrological survey at the southwestern coast of Taiwan, showing the significant influence of the fresh SGD at the coastal region of the Pingtung Plain, especially after a typhoon-induced flood event [*Peng et al.*, 2008; *Lin et al.*, 2010]. The enhanced SGD fluxes can be attributed to rapid responses of shallow and deep aquifers to the heavy rainfall event [*Oliveira et al.*, 2006].

[24] To quantify the fresh SGD fraction, a given water sample requires information on the properties of the freshwater end-member (in this case, the groundwater component near the KPE). Adapted average values of $^{87}Sr/^{86}Sr$ and the Sr content ($^{87}Sr/^{86}Sr$ = 0.712787, [Sr] = 5.7 μM and S = 2.3 (K.-F. Huang et al., unpublished data, 2011)) of groundwater samples from the deep aquifers of the Pingtung Plain and the seawater component ($^{87}Sr/^{86}Sr$ = 0.709187, [Sr] = 85.9 μM and S = 34.38, adopted from 400 m water depth of station 11, which is distant from the estuary) represent the fresh SGD and seawater end-member values, respectively. Based on the mass balance calculation, we can systematically determine how much fresh SGD would be necessary to produce the observed salinity in the deep water according to the equations (3) and (4):

$$S_S = S_{SGD} * f_{SGD} + S_{SW} * (1 - f_{SGD}) \quad (3)$$

$$\left(^{87}Sr/^{86}Sr\right)_S = \left(^{87}Sr/^{86}Sr\right)_{SGD} * f_{SGD} + \left(^{87}Sr/^{86}Sr\right)_{SW} * (1 - f_{SGD}) \quad (4)$$

where S_S is the salinity of unknown saline water, S_{SGD} is the salinity of the SGD end-member (S_{SGD} = 2.3), S_{SW} is the salinity of regional seawater end-member (S_{SW} = 34.38), and f_{SGD} is the mixing ratio of SGD to regional seawater in a sample. At station 3, a value of f_{SGD} at 470 m (S = 34.18) is estimated to be around 0.6%, which is identical to the fraction of fresh SGD estimated from the mass balance calculation using the seawater Sr isotope (~0.6%), indicating that the SGD contributes ~0.6% of the water in the KPC region. Again, this simplified mass balance calculation strongly supports the potential utilization of seawater Sr IC as a novel tracer for fresh SGD in the coastal region.

4.6. Uncertainties in Estimating the Saline and Freshwater Composition

[25] The above water mass composition analysis of the saline NPTW and the fresh SGD, based on the simple mass balance calculation (equation (1)–(4)), relies on choosing appropriate end-member values, which must reflect the bulk water properties (i.e., salinity and Sr isotope) of source regions. The main errors most likely arise in the determination of salinity and Sr IC in the seawater, as well as the possible seasonal variation in source water composition.

[26] The uncertainties about the errors in determining the salinity and seawater Sr IC can be further evaluated. Table 3 lists the result of the comparison in terms of the R_{mix} values (saline NPTW) between the salinity and Sr IC-based calculations at the upper 200 m of the SOT. According to the analytical precisions for salinity (±0.01) and seawater Sr IC (±3 ppm, 2σ), the errors for the estimated R_{mix} are ±0.09 and ±0.04 for salinity and Sr IC-based R_{mix}, respectively. In addition, applying the same approach, the uncertainties of f_{SGD} estimated from salinity and seawater Sr IC are ±0.0003 and ±0.0007, respectively. Taking the uncertainties into account, the calculated mixing ratios based on salinity and the seawater Sr IC are in agreement with each other. Based on these two independent approaches, we therefore conclude that seawater Sr IC can be used as a reliable indicator for tracing water mass mixing in the coastal ocean.

[27] Without more detailed information on the seasonal variability of source water composition, a more reliable and quantitative analysis of SGD is unwarranted. In this study, the saline waters (i.e., NPTW and SSW) can be inferred to have relatively little variation in terms of the physical and chemical properties of the seawater components. In contrast, there can be considerable variation in the chemical composition of shallow groundwater between dry and wet seasons, caused by mixing with deep groundwater and soil water in the discharge areas [*Land and Öhlander*, 1997]. In the deep KPC (~400–700 m), the freshwater component is most likely attributed from the deep groundwater of the Pingtung Plain [*Lin et al.*, 2010]. Although no hydrological and geochemical time series are available for the Pingtung Plain, the temporal variation should be relatively constant in the deep groundwater [*Land et al.*, 2000]. A more complete suite of measurements on temporal variations of deep groundwater composition in the Pingtung Plain should improve the accuracy of the mass balance calculation.

5. Concluding Remarks

[28] This study provides the first detailed investigation of seawater Sr IC vertical profiles in the

coastal ocean around western Pacific. Combining the results of Sr IC and S, we have found that the Sr IC distribution of the coastal waters is rather complicated and exhibits a nonhomogeneous vertical pattern (Δ^{87}Sr variation >70 ppm) around Taiwan, as well as two reference sites in the central SCS and Pacific. Surface enrichment in ^{87}Sr (more radiogenic Δ^{87}Sr) is attributed to the input of long-range transport of eolian dust from eastern Asia. The linear correlation between seawater Sr ICs and salinity in the upper 200 m of the SOT clearly indicates a two end-member mixing process occurred in the study area, characterized by a more radiogenic Sr IC water with high salinity (~100 m, NPTW) and a less radiogenic subsurface component (SSW) with low salinity at depth 200 m. Due to the limited change in salinity (<0.12) around the SOT, seawater Sr IC serves as a sensitive (total variation >70 ppm) and powerful tool for tracing the dynamic mixing processes of water masses and their migration pathway, especially in the coastal ocean and marginal sea.

[29] Vertical Δ^{87}Sr profiles along the KPC show large isotopic variations in the uppermost 200 m after a typhoon event, possibly affected by continental runoff and local seawater masses. Below 200 m, Sr IC gradually becomes more radiogenic toward the river mouth, reflecting the contribution of terrestrial inputs. Two radiogenic Sr layers found at intervals of 400–700 m and 1200 m are attributed to the potential influence of SGD after an episodic flood event. Simple isotopic mass balance calculations further support the application of seawater Sr isotopes for tracing the water mass mixing and freshwater input in the coastal oceans.

Acknowledgments

[30] We are grateful to C.-A. Huh, H.-L. Lin, S. Luo, W.-C. Chou, and C.-C. Su for collecting seawater samples. S.-F. Wu is appreciated for technical support in trace element measurements. S. Sosdian (Cardiff University) and J. Shakun (Boston University) are thanked for making the English more readable. This work was significantly improved by the constructive comments of anonymous reviewers and Editor Joel Baker. This research was supported by a postdoctoral fellowship from Top University (NCKU), Taiwan, to K.-F. Huang and funds from NSC and MOE, Taiwan, to C.-F. You.

References

Amakawa, H., Y. Nozaki, D. S. Alibo, J. Zhang, K. Fukugawa, and H. Nagai (2004), Neodymium isotopic variations in northwest Pacific waters, *Geochim. Cosmochim. Acta*, *68*, 715–727, doi:10.1016/S0016-7037(03)00501-5.

Amakawa, H., K. Sasaki, and M. Ebihara (2009), Neodymium isotopic composition in the central North Pacific, *Geochim. Cosmochim. Acta*, *73*, 4705–4719, doi:10.1016/j.gca.2009.05.058.

Andersson, P. S., G. J. Wasserburg, J. Ingri, and M. C. Stordal (1994), Strontium, dissolved particulate loads in fresh and brackish waters: The Baltic Sea and Mississippi Delta, *Earth Planet. Sci. Lett.*, *124*, 195–210, doi:10.1016/0012-821X(94)00062-X.

Basu, A. R., S. B. Jacobsen, R. J. Poreda, C. B. Dowling, and P. K. Aggarwal (2001), Large groundwater strontium flux to the oceans from the Bengal Basin and the marine strontium isotope record, *Science*, *293*, 1470–1473, doi:10.1126/science.1060524.

Bernstein, R. E., P. R. Betzr, R. A. Feely, R. H. Byrne, M. F. Lamb, and A. F. Michaels (1987), Acantharian fluxes and strontium to chlorinity ratios in the North Pacific Ocean, *Science*, *237*, 1490–1494, doi:10.1126/science.237.4821.1490.

Bernstein, R. E., R. H. Byrne, P. R. Betzr, and A. M. Greco (1992), Morphologies and transformations of celestite in seawater: The role of acantharians in strontium and barium geochemistry, *Geochim. Cosmochim. Acta*, *56*, 3272–3279.

Bickle, M. J., J. Bunbury, H. J. Chapman, N. B. W. Harris, I. J. Fairchild, and T. Ahmad (2003), Fluxes of Sr into the headwaters of the Ganges, *Geochim. Cosmochim. Acta*, *67*, 2567–2584.

Brass, G. W., and K. K. Turekian (1974), Strontium distributions in GEOSECCS oceanic profiles, *Earth Planet. Sci. Lett.*, *23*, 141–148, doi:10.1016/0012-821X(74)90041-7.

Burke, W. H., R. E. Denison, E. G. Hetherington, R. B. Koepnick, H. F. Nelson, and J. B. Otto (1982), Variations of seawater ^{87}Sr/^{86}Sr throughout Phanerozoic time, *Geology*, *10*, 516–519, doi:10.1130/0091-7613(1982)10<516:VOSSTP>2.0.CO;2.

Capo, R. C., and D. J. DePaolo (1992), Homogeneity of Sr Isotopes in the Oceans, *Eos Trans. AGU*, *73*, 272.

Chen, C. T. A., R. Ruo, S. C. Pai, C. T. Liu, and G. T. F. Wong (1995), Exchange of water masses between the East China Sea and the Kuroshio off northeastern Taiwan, *Cont. Shelf Res.*, *15*, 19–39, doi:10.1016/0278-4343(93)E0001-O.

Chen, C. T. A., S.-L. Wang, W.-C. Chou, and D. D. Sheu (2006), Carbonate chemistry and projected future changes in pH and $CaCO_3$ saturation state of the South China Sea, *Mar. Chem.*, *101*, 277–305, doi:10.1016/j.marchem.2006.01.007.

Chou, W.-C., D. D. Sheu, B. S. Lee, C. M. Tseng, C. T. A. Chen, S. L. Wang, and G. T. F. Wong (2007), Depth distributions of alkalinity, TCO_2 and $\delta^{13}C_{TCO2}$ at SEATS time-series site in the northern South China Sea, *Deep Sea Res., Part II*, *54*, 1469–1485, doi:10.1016/j.dsr2.2007.05.002.

Deniel, C., and C. Pin (2001), Single-stage method for the simultaneous isolation of lead and strontium from silicate samples for isotopic measurements, *Anal. Chim. Acta*, *426*, 95–103, doi:10.1016/S0003-2670(00)01185-5.

de Villiers, S. (1999), Seawater strontium and Sr/Ca variability in the Atlantic and Pacific oceans, *Earth Planet. Sci. Lett.*, *171*, 623–634, doi:10.1016/S0012-821X(99)00174-0.

Dia, A. N., A. S. Cohen, R. K. O'Nions, and N. J. Shackleton (1992), Seawater Sr- isotope variations over the last 300 kyr and global climate change, *Nature*, *356*, 786–788, doi:10.1038/356786a0.

Henderson, G. M., D. J. Martel, R. K. O'Nions, and N. J. Shackleton (1994), Evolution of seawater ^{87}Sr/^{86}Sr over the past 400 ka: The absence of glacial/interglacial cycles, *Earth Planet. Sci. Lett.*, *128*, 643–651, doi:10.1016/0012-821X(94)90176-7.

Huang, K.-F., and C.-F. You (2007), Tracing freshwater plume migration in the estuary after a typhoon event using Sr isotopic ratios, *Geophys. Res. Lett.*, *34*, L02403, doi:10.1029/2006GL028253.

Jacobson, A. D. (2004), Has the atmospheric supply of dissolved calcite dust to seawater influenced the evolution of marine $^{87}Sr/^{86}Sr$ ratios over the past 2.5 million years?, *Geochem. Geophys. Geosyst.*, *5*, Q12002, doi:10.1029/2004GC000750.

Land, M., and B. Öhlander (1997), Seasonal variations in the geochemistry of shallow groundwater hosted in granitic till, *Chem. Geol.*, *143*, 205–216, doi:10.1016/S0009-2541(97)00116-2.

Land, M., J. Ingri, P. S. Andersson, and B. Öhlander (2000), Ba/Sr, Ca/Sr and $^{87}Sr/^{86}Sr$ ratios in soil water and groundwater: Implications for relative contributions to stream water discharge, *Appl. Geochem.*, *15*, 311–325, doi:10.1016/S0883-2927(99)00054-2.

Lin, I.-T., C.-H. Wang, C.-F. You, S. Lin, K.-F. Huang, and Y.-G. Chen (2010), Deep submarine groundwater discharge indicated by tracers of oxygen, strontium isotopes and barium content in the Pingtung coastal zone, southern Taiwan, *Mar. Chem.*, *122*, 51–58, doi:10.1016/j.marchem.2010.08.007.

Moore, W. S. (1996), Large groundwater inputs to coastal waters revealed by ^{226}Ra enrichments, *Nature*, *380*, 612–614, doi:10.1038/380612a0.

Moore, W. S. (1997), High fluxes of radium and barium from the mouth of the Ganges-Brahmaputra River during low river discharge suggest a large groundwater source, *Earth Planet. Sci. Lett.*, *150*, 141–150, doi:10.1016/S0012-821X(97)00083-6.

Nitani, H. (1972), Beginning of the Kuroshio, in *Kuroshio*, edited by H. Stommel and Y. Yoshida, pp. 129–163, Univ. of Wash. Press, Seattle.

Oliveira, J., P. Costa, and E. S. Braga (2006), Seasonal variation of ^{222}Rn and SGD fluxes to Ubatuba embayments, São Paulo, *J. Radioanal. Nucl. Chem.*, *269*, 689–695, doi:10.1007/s10967-006-0287-2.

Peng, T.-R., C.-T. A. Chen, C.-H. Wang, J. Zhang, and Y.-J. Lin (2008), Assessment of terrestrial factors controlling the submarine groundwater discharge in water shortage and highly deformed island of Taiwan, western Pacific ocean, *J. Oceanogr.*, *64*, 323–337, doi:10.1007/s10872-008-0026-0.

Qu, T., H. Mitsudera, and T. Yamagata (2000), Intrusion of the North Pacific waters into the South China Sea, *J. Geophys. Res.*, *105*(C3), 6415–6424, doi:10.1029/1999JC900323.

Reid, J. L. (1997), On the total geostrophic circulation of the Pacific Ocean: Flow patterns, tracers, and transports, *Prog. Oceanogr.*, *39*, 263–352, doi:10.1016/S0079-6611(97)00012-8.

Robb, J. M. (1984), Spring sapping on the lower continental slope, offshore New Jersey, *Geology*, *12*, 278–282, doi:10.1130/0091-7613(1984)12<278:SSOTLC>2.0.CO;2.

Schauble, E. A. (2004), *Geochemistry of Non-Traditional Stable Isotopes*, *Rev. in Mineral. and Geochem.*, 55, 65–102 p., The Mineralogical Society of America.

Stoll, H. M., and D. P. Schrag (1998), Effects of Quaternary sea level cycles on strontium in seawater, *Geochim. Cosmochim. Acta*, *62*, 1107–1118, doi:10.1016/S0016-7037(98)00042-8.

Tomczak, M., and J. S. Godfrey (1994), *Regional Oceanography: An Introduction*, 422 pp., Pergamon, Oxford, U. K.

Winter, B. L., D. L. Clark, and C. M. Johnson (1997), Late Cenozoic Sr isotope evolution of the Arctic Ocean: Constraints on water mass exchange with the lower latitude oceans, *Deep Sea Res., Part II*, *44*, 1531–1542, doi:10.1016/S0967-0645(97)00053-2.

Xu, Y., and F. Marcantonio (2004), Speciation of strontium in particulates and sediments from the Mississippi River mixing zone, *Geochim. Cosmochim. Acta*, *68*, 2649–2657, doi:10.1016/j.gca.2003.12.016.

You, Y. (2003), The pathway and circulation of North Pacific Intermediate Water, *Geophys. Res. Lett.*, *30*(24), 2291, doi:10.1029/2003GL018561.